

# Resveratrol Reduces the Invasive Growth and Promotes the Acquisition of a Long-Lasting Differentiated Phenotype in Human Glioblastoma Cells

Roberta Castino,<sup>\*,†</sup> Anja Pucer,<sup>\*,†,‡</sup> Roberta Veneroni,<sup>†</sup> Federica Morani,<sup>†</sup> Claudia Peracchio,<sup>†</sup> Tamara T. Lah,<sup>‡</sup> and Ciro Isidoro<sup>\*,†</sup>

<sup>†</sup>Laboratorio di Patologia Molecolare, Dipartimento di Scienze Mediche, Università del Piemonte Orientale A. Avogadro, 28100 Novara, Italy

<sup>‡</sup>Department of Genetic Toxicology and Cancer Biology, National Institute of Biology, and Faculty of Chemistry and Chemical Technology, University of Ljubljana, SI-1000 Ljubljana, Slovenia

**ABSTRACT:** Malignant glioblastoma represents a challenge in the chemotherapy of brain tumors, because of its aggressive behavior characterized by chemoresistance, infiltrative diffusion, and high rate of recurrence and death. In this study, we used cultured human U87MG cells and primary human glioblastoma cultures to test the anticancer properties of resveratrol (RV), a phytoalexin abundantly present in a variety of dietary products. In U87MG cells, 100  $\mu$ M RV elicited cell growth arrest by 48 h and bax-mediated cell toxicity by 96 h and greatly limited cell migration and invasion through matrigel. Both in U87MG cells and in primary glioblastoma cultures, the chronic administration of RV (100  $\mu$ M for up to 96 h) decreased the expression of nestin (a brain (cancer) stem cells marker) but increased that of glial acidic fibrillary protein (a mature glial cell marker) and of  $\beta$ III-tubulin (a neuronal differentiation marker). Chronic treatment with RV increased the proportion of cells positive for senescence-associated  $\beta$ -galactosidase activity. This is the first report showing the ability of RV to induce glial-like and neuronal-like differentiation in glioblastoma cells. The beneficial effects of chronic RV supplementation lasted up to 96 h after its withdrawal from the culture medium. The present findings support the introduction of pulsed administration of this food-derived molecule in the chemotherapy regimen of astrocytomas.

**KEYWORDS:** Resveratrol, cancer, apoptosis, glioma, tumor invasion, cancer stem cells

## INTRODUCTION

Glioblastoma (GBM, grade IV astrocytoma) is the most malignant form of brain tumors, characterized by intense proliferation, chemoresistance, invasion, and recurrence.<sup>1</sup> A basal high level of (ser473)phosphorylated Akt, often associated with loss of the oncosuppressor PTEN, has been associated with maintenance and self-renewal of stem cells and invasiveness in GBM<sup>2</sup> and with poor prognosis in GBM-bearing patients.<sup>3</sup> Cancer stem-like cells from infiltrative human glioblastoma have been shown highly resistant to cell therapy.<sup>4</sup> Thus, a more efficacious strategy to cure glioblastomas could include in the therapy regimen drugs able to induce a differentiated and mature phenotype of cancer cells that may have lower resistance to chemotherapeutics or radiotherapy.

Resveratrol (3,4',5-trihydroxy-*trans*-stilbene, RV), a phytoalexin naturally present in grapes, red wine, multiberries, peanuts, and other dietary products, has recently attracted the interest of experimental and clinical oncologists because of its anticarcinogenic properties demonstrated in several *in vivo* cancer models.<sup>5–8</sup> *In vitro* studies on human tumor cells have shown that RV inhibits cell cycle progression,<sup>9</sup> migration, and invasion through a synthetic matrix<sup>10</sup> and induces apoptosis.<sup>11,12</sup> RV cytotoxicity in cancer cells has been shown to also involve an autophagy pathway.<sup>13,14</sup> Absorption, bioavailability, and pharmacokinetic studies on RV orally administered at high doses to healthy volunteers have confirmed that this drug is safe and well tolerated,<sup>15,16</sup> thus supporting its potential utilization in cancer chemotherapy.

In this work, we show that RV not only exerts antiproliferative and anti-invasive effects, but it also induces a senescence-like growth arrest and the acquisition of a long-lasting more mature phenotype in human glioblastoma cells. This is the first report showing the ability of RV to induce glial-like and neuronal-like differentiation in glioblastoma cells.

## MATERIALS AND METHODS

**Source and Culture of U87MG Cells and of Primary Glioblastoma Cells.** Human glioblastoma U87MG cells were obtained from the American Type Culture Collection (Manassas, VA) cultured under standard conditions (37 °C in humidified atmosphere with 5% CO<sub>2</sub>) as a monolayer in DMEM medium (Sigma-Aldrich, St. Louis, MO) supplemented with 10% fetal bovine serum (FBS), 1% nonessential amino acids, 1% penicillin/streptomycin, 2.5 mM L-glutamine (PAA Laboratories, Linz, Austria).<sup>17</sup>

Human primary GBM cells were isolated from two WHO grade IV glioblastoma explants obtained at the Department of Neurosurgery, University Clinical Centre of Ljubljana.<sup>18</sup> Cells were grown in DMEM/F12 (Sigma-Aldrich) supplemented with 10% FBS, 2 mM L-Gln, 1x Pen/Strep (all from PAA Laboratories), and 0.01 M HEPES (Sigma-Aldrich). Cells at passage 9 were used for experiments presented in this study.

**Received:** December 23, 2010

**Accepted:** February 14, 2011

**Revised:** February 11, 2011

**Published:** March 11, 2011

**Assessment of Resveratrol Effect on Cell Morphology, Cell Cycle, and Cell Death.** Cells were plated and allowed to adhere at least 24 h prior to start the treatment with 10–200  $\mu\text{M}$  RV (*trans*-3,4',5-trihydroxystilbene; Sigma-Aldrich) for 24–96 h. RV was dissolved in DMSO (Sigma-Aldrich) at 100 mM stock concentration. The vehicle DMSO was present in control and treated cultures at a maximum final concentration of 0.2%. Morphological changes were documented by imaging the monolayers under a phase-contrast microscope. Cell growth and occurrence of cell death were assessed by counting viable (trypan blue-excluding) cells and by cytofluorometry analysis of cells labeled with annexin V-FITC and propidium iodide (in the latter case, adherent cells were collected by trypsinization and pooled with floating cells before analysis).<sup>14</sup> For cell cycle analysis, the cells were washed in PBS and fixed in 70% EtOH at 4 °C overnight. Fixed cells were washed once in PBS, resuspended in PBS+RNase (100  $\mu\text{g}/\text{mL}$ ), and incubated at 37 °C for 1 h. Finally, 5 mM EDTA/PBS and propidium iodide (final concentration 50  $\mu\text{g}/\text{mL}$ ) were added. Cells were analyzed on a Becton Dickinson FACS SCAN. Data were acquired with CellQuest software (10000 gated events/sample, doublet exclusion with DDM on FL-2) and analyzed with WinMDI 2.9 and Cylchred.

**Fluorescence Imaging of Antigens, Nuclei, and Mitochondria.** Cells were plated on sterile coverslips, and, after treatments, they were fixed in methanol or paraformaldehyde and processed for immunofluorescence.<sup>12</sup> The integrity of mitochondrial membrane was demonstrated by retention of the fluorescent probe mitotracker (Molecular Probes-Invitrogen Co S.R.L., Milan, Italy). At the end of the treatment, the cells were incubated for 1 h at 37 °C with 100 nM mitotracker and then fixed (in 3.7% paraformaldehyde) and processed for immunofluorescence detection of bax with an antibody directed to the conformationally active form (Cell Signaling Technology, Danver, MA). Nuclei were evidenced by chromatin staining with DAPI (Sigma-Aldrich). Differentiation-associated antigens were detected using antibodies specific for nestin, GFAP, and  $\beta$ III tubulin (Chemicon, Millipore, Billerica MA). Ki67 staining was performed with either rabbit polyclonal anti-Ki67 (Abcam plc, Cambridge, UK) or mouse monoclonal anti-Ki67 (Dako Cytomation, Glostrup, Denmark). As secondary antibodies, either IRIS-2 (green fluorescence)- or IRIS-3 (red fluorescence)-conjugated goat-antirabbit IgG or goat-antimouse IgG (Cyanine Technology SpA, Turin, Italy) were used as appropriate. Images were captured with the fluorescence microscopes Nikon Eclipse E800 and Leica DM1600. All experiments were replicated at least three times.

**Invasion Assay in Matrigel-Coated Modified Boyden Chambers.** The upper surface of chambers (12-well polycarbonate filter inserts with 12  $\mu\text{m}$  pores, Sigma-Aldrich) was coated with Matrigel (50  $\mu\text{g}/\text{well}$ , Becton Dickinson, Franklin Lakes, NJ) in serum free medium. The filters were dried overnight and reconstituted with 0.2 mL of medium ( $\pm 100 \mu\text{M}$  RV) 1 h prior to cell seeding. Cells were detached using 0.4% EDTA/0.1% BSA/PBS and seeded on the upper chamber at a density of 100 000 cells/well in 0.5 mL medium, and 1.5 mL of medium was added in the lower chamber. In RV-treated cells, RV was added to both upper and lower chambers, at a final concentration of 100  $\mu\text{M}$ . The cells were then incubated at 37 °C for 48 h with medium ( $\pm 100 \mu\text{M}$  RV) change after the first 24 h. At the end, MTT (Sigma-Aldrich) at 0.5 mg/mL final concentration was added to both chambers. After 1 h, the formazan crystals were collected separately from the upper and lower chambers, sedimented by centrifugation and dissolved in 1 mL of DMSO. Absorbance (assumed as proportional to viable cell number) was measured at 570 nm (reference filter 690 nm) with a GENios spectrofluorometer (Tecan, Salzburg, Austria). Invasion was calculated as the ratio of the number of cells in the lower compartment to the sum of cells in both compartments. The mean invasion of two independent experiments (each performed in triplicates) is shown.

**Wound-Healing Assay.** To test cell migration, a classical *in vitro* "wound healing assay" was employed. In brief, U87MG cells were grown in culture Petri dishes to approximately 80% confluence, and then a

wound was made by dragging a needle along the center of the plate. Detached cells were washed out twice, and cultures were incubated in fresh medium containing RV or not. Photographs were taken at the time indicated under the phase-contrast microscope. Two investigators, blind to the treatment, independently calculated the wound wideness by measuring the mean distance between the margins of the wound in randomly selected fields, directly on photographs. Overall, four independent experiments were performed.

**Immunoblotting.** Immunoblotting was performed following standard procedures. Akt and (ser473)-phosphorylated Akt were detected with specific rabbit polyclonal antihuman Akt antisera (Cell Signaling Technology). p21<sup>WAF/cip1</sup> was detected with a monoclonal antihuman antibody (Santa Cruz Biotechnology, CA). The same filter was subsequently probed with a mouse monoclonal antibody specific for  $\beta$ -actin (Sigma-Aldrich) to prove equal loading of homogenate proteins between lanes. Immunocomplexes were revealed by using a peroxidase-conjugated secondary antibody, as appropriate, and subsequent peroxidase-induced chemiluminescence reaction (BIO-RAD Laboratories, Milan, Italy). Western blotting data were reproduced in three separate experiments (one representative gel is shown). Intensity of the bands was estimated by densitometry (Quantity one software, BIO-RAD Laboratories).

**mRNA Expression Analysis by qRT-PCR.** RNA was isolated with TRIzol reagent (GIBCO Products, Invitrogen, Grand Island NY) and quantified on a NanoDrop ND-1000 spectrophotometer (NanoDrop Technologies Inc., Wilmington, DE), and 1.0  $\mu\text{g}$  of each RNA sample was reverse transcribed to cDNA using High Capacity cDNA Reverse Transcription Kit (Applied Biosystems, Foster City CA). Quantitative real-time-PCR (qRT-PCR) was performed on ABI Prism 7900 HT Sequence Detection System using TaqMan Universal PCR Master Mix, human GAPDH as internal control and predesigned primers for nestin (Hs00707120\_s1), GFAP (Hs00157674\_m1), and  $\beta$ III tubulin (Hs00801390\_s1) (all Applied Biosystems). Fold increase in mRNA levels was calculated using the Delta-delta ct method ( $2^{-(\Delta\text{ct}_{\text{treated}} - \Delta\text{ct}_{\text{notreated}})}$ );  $\Delta\text{ct} = \text{ct}_{\text{gene}} - \text{ct}_{\text{GAPDH}}$ ) and presented as mean of three independent experiments.

**Senescence-Associated  $\beta$ -Galactosidase Staining.** Cells grown on poly-L-lysine-coated coverslips were treated for 96 h with medium ( $\pm 100 \mu\text{M}$  RV) change at every 24 h and fixed in freshly prepared 0.2% glutaraldehyde/PBS for 5 min, washed in PBS, and incubated with senescence-associated  $\beta$ -galactosidase staining solution (senescence-associated  $\beta$ -galactosidase staining solution: 40 mM citric acid/sodium phosphate, pH 6.0, containing 1 mg/mL Xgal (5-bromo-4-chloro-3-indolyl- $\beta$ -galactopyranoside, Sigma-Aldrich), 5 mM potassium ferrocyanide, 5 mM potassium ferricyanide 150 mM NaCl, and 2 mM  $\text{MgCl}_2$ ) overnight at 37 °C (without  $\text{CO}_2$ ). Directly before observation, nuclei were counterstained with Hoechst (Invitrogen), for total cells count, and cells were observed with the Nikon Eclipse E800 fluorescence microscope equipped with a mercury lamp and UV filter (330–380 nm excitation and >420 nm emission) and visible light lamp. At least 200 total cells per condition were counted, and cells with intensive perinuclear blue visible light staining were determined as  $\beta$ -gal<sup>+</sup> cells.

**Statistical Analysis.** All experiments were reproduced at least three times in double or in triplicate (unless otherwise specified). Data were expressed as mean value  $\pm$  SD. Student's *t* test (two-tailed, unpaired assuming equal variances) was used to calculate statistically significant differences between control and RV-treated samples. Results with  $p < 0.05$  were considered statistically significant.

**Ethics.** The study on human primary glioblastomas was approved on 10.07.2009 by the Slovene Committee for Ethics in Medical Research, in conformity to local legislation and the Helsinki Declaration.

## RESULTS

**Chronic Treatment with Resveratrol Affects Cell Proliferation and Morphology in U87MG Cultures.** U87MG cells were

exposed for up to 4 days to increasing concentrations (10, 50, 100, and 200  $\mu\text{M}$ ) of RV. RV was readded daily with fresh medium. As judged by microscopy observation, RV slowed cell proliferation and promoted the appearance of elongated cytoplasmic extensions (Figure 1A). These effects were dose- and time-dependent, being more evident by days 3 and 4, and at  $>50 \mu\text{M}$  concentration. Induction of cell death by RV was assayed by cytofluorometry of cells treated as above and double-labeled with propidium iodide (PI) and annexin V-FITC. In nonfixed cells PI enters only cells with permeabilized plasma membrane, and therefore PI-positive cells are considered necrotic. Positivity to annexin V was assumed bona fide as indicative of apoptotic cell death. Up to 200  $\mu\text{M}$  RV was not toxic to U87MG cells in the first 24 h (not shown). In line with a dose- and time-dependency of RV effect on cell survival, 100  $\mu\text{M}$  RV was revealed to be slightly toxic by 48 h and induced 38 ( $\pm 2$ ) % annexin V-positive cell death by 96 h, whereas 10  $\mu\text{M}$  RV elicited limited toxicity only at 96 h (Figure 1B). The activation of the intrinsic death pathway was assessed by double-staining the cells with mitotracker (a tracer of mitochondrial membrane integrity) and with antibodies specific for the conformational active bax. A 100  $\mu\text{M}$  concentration of RV triggered the bax-mediated permeabilization of mitochondria in U87MG cells, the effect becoming more pronounced after 48 h of treatment (Figure 1C). On the basis of these data, we conclude that the prolonged treatment with 100  $\mu\text{M}$  RV induced the activation of the intrinsic death pathway but did not cause necrosis. For the next experiments, aimed to investigate the biological effects of RV on U87MG cells, the concentration of 100  $\mu\text{M}$  was chosen. U87MG cells were plated at the initial density of 15 000 cells/ $\text{cm}^2$ , and the treatment started 24 h later (time 0), at which time-point cell density had reached approximately 25 000 cells/ $\text{cm}^2$  (Figure 2A). Cells were cultured, renewing the culture medium every 24 h in order to avoid side-effects of nutrient and growth factors consumption, and RV was readded daily. In control cultures, cells reproduced with a doubling time of approximately 27 h (Figure 2A). In cultures exposed to 100  $\mu\text{M}$  RV, cell growth was slowed in the first 48 h, and after this time-point, cell loss became apparent (Figure 2A). Ki-67 is a nuclear protein expressed in all phases, except for G0, of the cell cycle and is widely used in clinical routine to evaluate the proliferative activity of human astrocytomas.<sup>19</sup> We calculated the percentage of Ki-67-positive cells in control and 100  $\mu\text{M}$  RV-treated (48 h) cultures, as a rough estimation of the inhibitory effect of RV on cell proliferation. At day 2 in control cultures, 37 ( $\pm 4$ ) % of the cells stained for Ki-67, whereas in RV-treated cultures, the percentage of Ki-67-positive cells dropped to 21 ( $\pm 8$ ) % (Figure 2B). Thus, by 48 h, 100  $\mu\text{M}$  RV reduced the proportion of proliferating cells by  $\sim 50\%$ . We further performed flow cytometry analysis of the cell cycle in U87MG cultures exposed for up to 3 days to 100  $\mu\text{M}$  RV. Representative cytofluorograms and their relative quantification are shown in Figure 2C and 2D, respectively. In control cultures, cells appear actively dividing and show, during the 3 days of cultivation, a progressive reduction of the fraction of cells in the S phase, paralleled by an increase of the fraction in the G2 phase. In RV-treated cultures, soon after 24 h the cells started to accumulate in the S phase of the cell cycle and by 72 h, this fraction further increased, while the proportion of cells in the G2 phase was greatly reduced. We observed more than 3-fold increase in the number of cells in the S phase after 72 h of RV treatment ( $\sim 45\%$  vs  $\sim 15\%$ ), with a concomitant reduction in the number of cells in G2/M phase ( $\sim 5\%$  vs  $\sim 45\%$ ), as compared with the respective control.

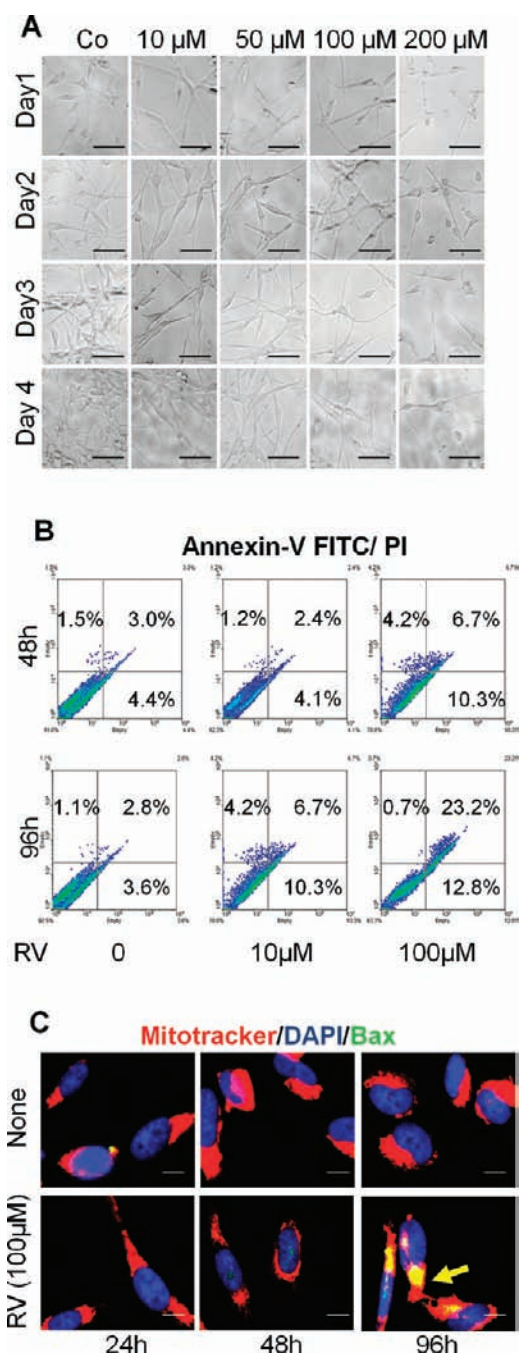


**Figure 1.** Dose- and time-dependent effect of resveratrol on cell morphology and cell death. Adherent U87MG cells were treated with resveratrol (RV) at the concentration and for the time indicated. (A) The monolayer was photographed under a phase-contrast microscope to document the morphological changes associated with the treatment (bar = 0.1 mm). (B) At the end of the incubation, the cells were colabeled with propidium iodide (PI) and annexin V-FITC and analyzed by cytofluorometry. Representative biparametric cytofluorograms are shown. The percentage of dead cells is indicated. Note: only PI-positive cells are referred to as primary necrotic; only annexin V-positive cells are referred to as apoptotic; double annexin V/PI-positive cells are referred to as apoptotic cells that underwent secondary necrosis. (C) The cells cultivated on sterile coverslips were treated as indicated and processed for fluorescence imaging of mitochondrial integrity (using the probe Mitotracker) and of bax activation (bar = 10  $\mu\text{m}$ ). Data shown in this figure were reproduced in three independent experiments.

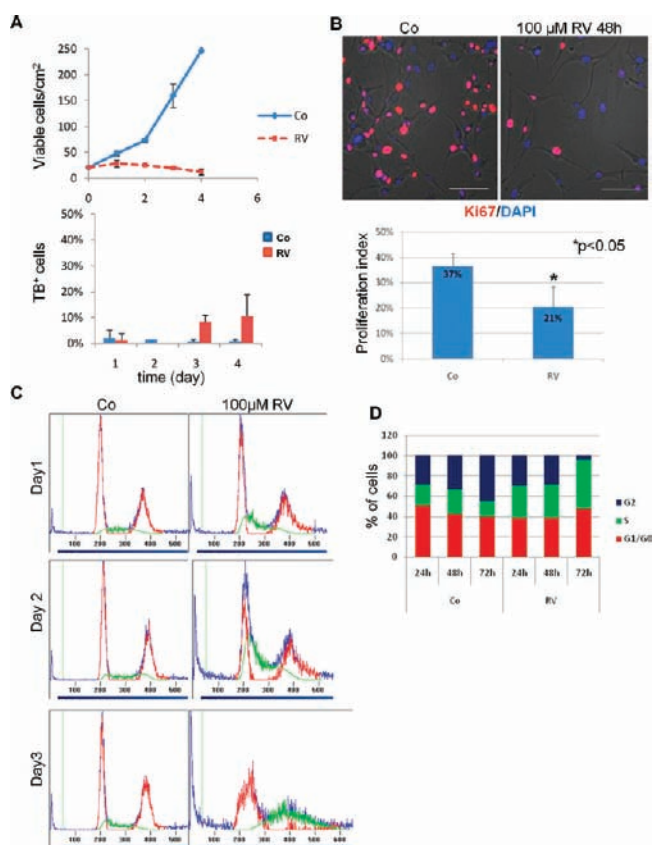


**Figure 2.** Effect of resveratrol on the viability and proliferation of U87MG cells. (A) Count of viable (upper panel) and trypan blue-positive necrotic (lower panel) U87MG cells exposed to 100  $\mu$ M RV for up to 96 h (average of three experiments in triple  $\pm$  SD). (B) Representative images (upper panel; bar = 0.1 mm) and quantification (lower panel; average of three experiments in triple  $\pm$  SD;  $p < 0.05$ ) of Ki-67 expression in U87MG cells exposed to 100  $\mu$ M RV for up to 48 h. Nuclei were counterstained with DAPI. (C and D) Cytofluorograms (panel C: the blue line shows the nonanalyzed histogram, the red line shows the G0/G1 and G2/M peaks, and the green line shows the S-phase after analysis) and quantification (panel D) of cell cycle analysis of U87MG cells exposed to 100  $\mu$ M RV for up to 72 h (representative data of three independent experiments are shown).

**Chronic Exposure to Resveratrol Reduces 'in Vitro' Migration and Invasiveness of U87MG Cells.** Next, we tested whether RV inhibits or reduces the invasive motility of U87MG cells by using the 'in vitro' matrigel invasion assay. The cells were seeded on the top of the matrigel-coated filter and cultured in the absence or the presence of 100  $\mu$ M RV for 48 h, then the number of cells persisting in the upper chamber and of those that passed the filter and attached to the lower chamber were evaluated. U87MG cells were revealed to be highly invasive, since as many as 42 ( $\pm$ 3) % of the initial population passed through the matrigel within the 48 h (Figure 3A). The number of vital cells that reached the bottom chamber was drastically reduced upon treatment with RV, accounting for 26 ( $\pm$ 3) % of the initial population (Figure 3A). Thus, a 48 h treatment with RV elicited some 48% reduction of the potential of U87MG cells to invade through the matrigel. We further investigated whether this outcome was the result of an inhibitory action of RV on the motility of U87MG cells. We employed the 'wound-healing' assay to test the potential ability of RV to inhibit cell migration.

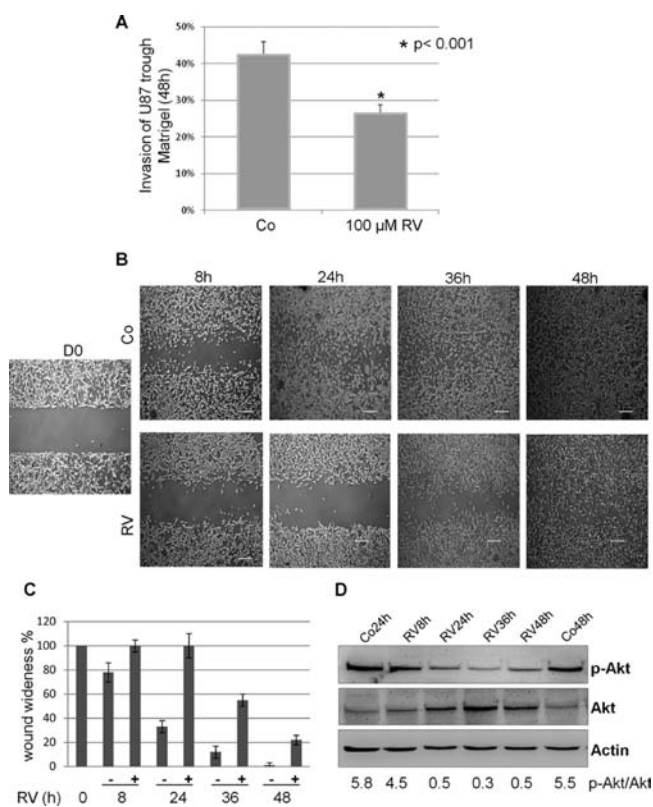


**Figure 3.** Effect of resveratrol on invasive and motility abilities of U87MG cells. (A) Inhibitory effect of RV on the ability of U87MG cells to migrate through a synthetic collagen matrix (data of two experiments in triple  $\pm$  SD;  $p < 0.001$ ). (B and C) Representative phase-contrast microscope images and quantification (average of three independent experiments  $\pm$  SD), respectively, of the inhibitory effect of RV on the motility of U87MG cells exposed to 100  $\mu$ M RV for up to 48 h in a classical wound-healing assay. (D) Expression of Akt and ser473-pAkt in control and RV-treated U87MG cells. Representative immunoblot (one out of three) showing the inhibitory effect of RV on the serphosphorylation of Akt. Densitometry ratio of pAkt vs Akt is reported. The same filter was also probed for actin expression as a protein homogenate loading control.

U87MG cells were seeded on plastic dishes and cultured until the cells reached a confluent state, and then cell layers were wounded with a disposable plastic micropipet tip. The medium and debris were aspirated away and replaced with fresh medium containing 100  $\mu$ M RV or not. Cultures were observed and photographed every 8–12 h. Phase-contrast microscope images of the monolayers (Figure 3B) document the inhibitory effect of RV on U87MG cell motility. Quantification of this effect is reported in Figure 3C. In control cultures, the cells at the opposite front of the wound promptly (in the first 8 h) moved toward each other, and this movement led to the complete healing of the wound by 48 h. By contrast, in RV-treated cultures this movement was greatly slower than in controls (the distance between the opposite fronts remained unchanged in the first 24 h), and the wound was still unhealed by 48 h. Activation of the Akt pathway has been shown to promote cell motility and tumor invasion,<sup>20</sup> and, consistently, migrating glioma cells have shown to possess increased levels of phosphorylated Akt.<sup>21</sup> We therefore investigated whether the inhibitory effect of RV on U87MG migration was due to modulation of the Akt signaling pathway. RV promptly and strongly down-regulated (approximately 10-fold

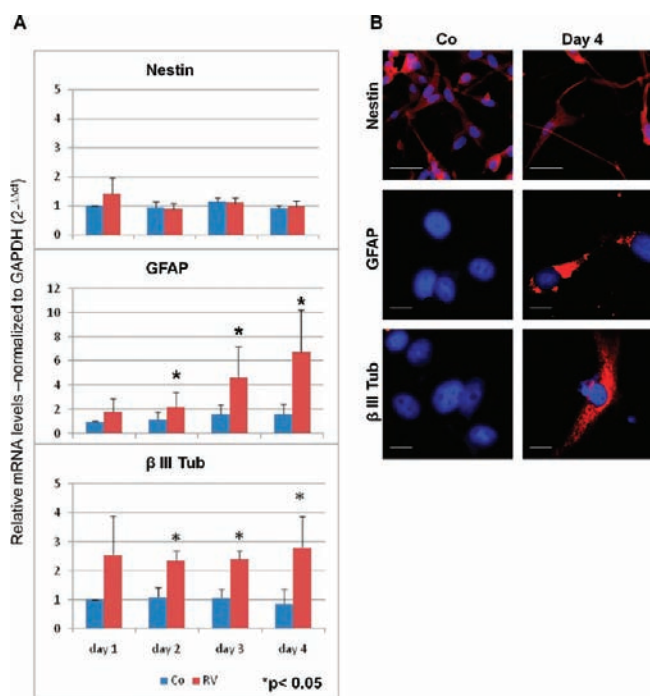


**Figure 4.** Effect of resveratrol on the expression of differentiation markers in U87MG cells. (A) U87MG cells were cultured for 96 h in the absence (Co) or the presence of 100  $\mu$ M resveratrol (RV). Medium was changed and RV readded every 24 h. At the time-points indicated, cells were collected and the expression of nestin, GFAP, and  $\beta$ III tubulin mRNAs was evaluated by qRT-PCR (data of three independent experiments  $\pm$  SD;  $p < 0.05$ ). (B) Representative images (of three independent experiments) of immunofluorescence expression of nestin (bar = 0.1 mm), GFAP (bar = 20  $\mu$ m), and  $\beta$ III tubulin (bar = 20  $\mu$ m) in U87MG cells treated with RV for 96 h.

decrease after 24 h of treatment) the (ser473)-phosphorylation of Akt, the effect being evident already at 8 h of treatment and sustained throughout the incubation (Figure 3D).

**Chronic Exposure to Resveratrol Induces Long-Lasting Expression of Differentiation Markers in U87MG Cells.** GBMs were shown to be composed of a mixture of immature cells containing, in a small percentage, brain cancer stem cells that have multilineage differentiation potency.<sup>22,23</sup> We asked whether the morphological and behavioral changes induced by RV in U87MG cells were associated with the acquisition of a more mature phenotype. The expression of certain markers is useful in the characterization of the differentiation status of glioma cells. Among these markers, nestin and prominin-1/CD133 are reportedly expressed in neural stem cells and in brain cancer stem cells.<sup>22,23</sup> CD133 is, however, expressed at a nondetectable level in cultured U87MG cells.<sup>24</sup> As markers for glial-like or neuronal-like maturation, we chose the glial fibrillary acidic protein (GFAP) and  $\beta$ III tubulin, respectively.<sup>25,26</sup> We performed quantitative real-time RT-PCR and immunofluorescence analyses to assess whether the chronic administration of RV influenced the expression of these markers. In RV-treated cells, the expression of nestin mRNA was down-regulated, after an initial (first 24 h) slight increase, to the level found in control cells (Figure 4A). RV promptly up-regulated the transcription level of  $\beta$ III tubulin gene, whose mRNA increased by 2.5-fold in the first 24 h and remained stable throughout the 96 h of incubation (Figure 4A). More interestingly, a 4 day treatment with RV resulted in a

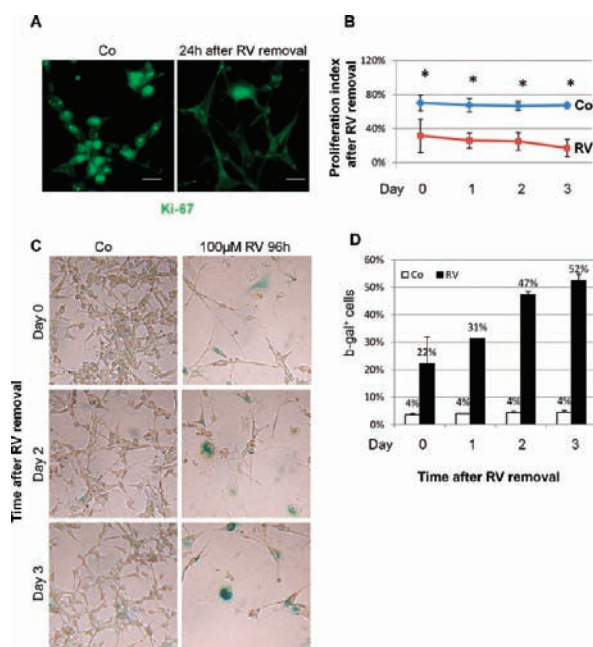


**Figure 5.** Resveratrol induces senescence-like growth arrest in U87MG cells. U87MG cells were treated for 96 h with 100  $\mu$ M RV (medium was changed and RV readded every 24 h), and then they were cultured in fresh medium (changed every 24 h) for the time indicated in the absence of RV. (A) Representative images of Ki-67 immunofluorescence staining taken at 24 h (bar = 0.1 mm). (B) Quantification of Ki-67 expression in U87MG cells cultured for up to 72 h after RV withdrawal. (C) Representative images of the cells stained for senescence-associated  $\beta$ -galactosidase activity. (D) At least 200 total cells per condition were counted, and cells with intensive perinuclear blue visible light staining were determined as  $\beta$ -galactosidase-positive cells; the mean value ( $\pm$ SD) of three independent experiments is shown in the diagram.

progressive increase of GFAP mRNA, which reached a level  $\sim$ 4.3-fold that of untreated cells (Figure 4A). Immunofluorescence staining of these markers confirmed the modulating effects of RV on their expression (Figure 4B). We then checked whether the above morphological and biochemical effects induced by RV persisted after removal of the drug from the culture medium. The morphology acquired by the cells that survived a 96 h treatment with RV was maintained for up to 3 days after RV withdrawal from the culture (compare the images in Figures 5 and 1). We also noted that, in chronically pretreated U87MG cultures, cell density did not increase during the 3 day culture without RV. In parallel cultures, we assessed the proliferation index by counting the Ki-67-positive cells (Figure 5A). The cells that survived to the chronic (96 h) treatment with RV did not rescue the ability to proliferate during the 3 day culture in RV-free medium (Figure 5B). We suspected that RV could have induced a senescence-like growth arrest and, therefore, checked for the presence of cells positive for senescence-associated  $\beta$ -galactosidase activity (Figure 5C). The proportion of cells expressing the lysosomal marker of cell senescence in cultures exposed for 96 h to RV and then cultured in fresh RV-free medium for up to 3 days increased from initial 22% to 52%, while in control unexposed cultures the percentage of cells positive for  $\beta$ -galactosidase remained at 4% (Figure 5D). Next, we looked at the expression of differentiation markers in these cultures. Data in Figure 6 show that in untreated cells the mRNA levels of nestin, GFAP, and  $\beta$ III-tubulin remained substantially unmodified during the 72 h of incubation,

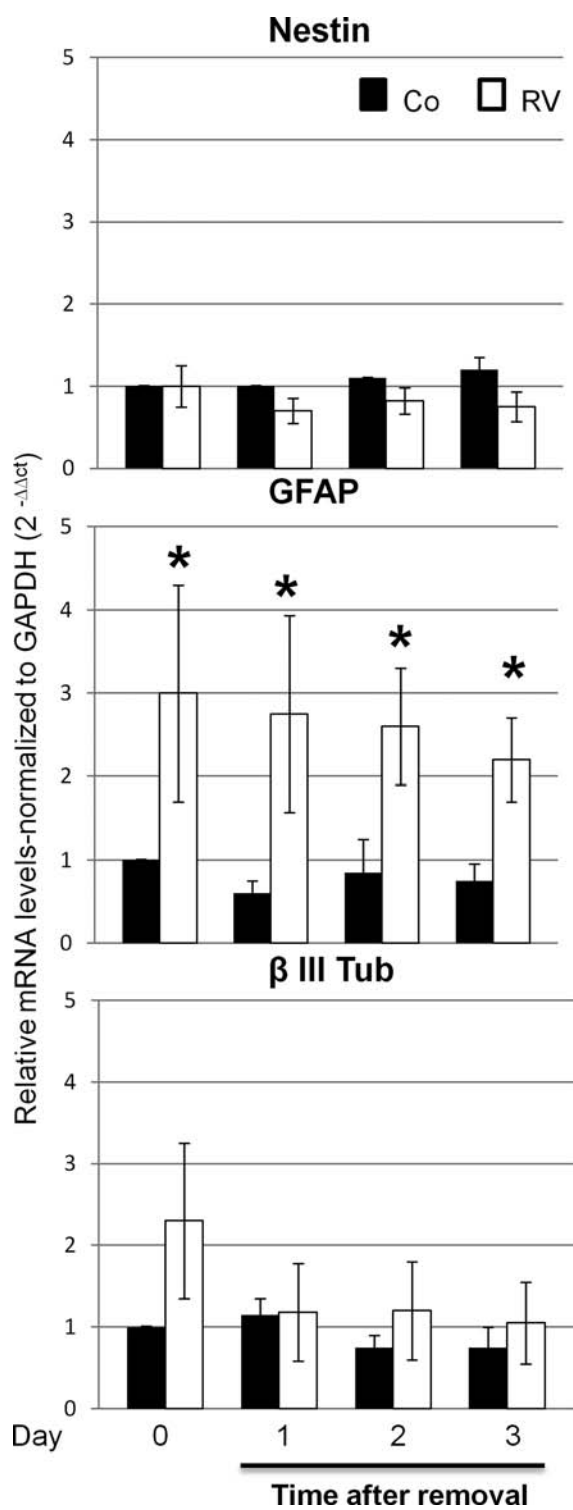


**Figure 6.** Resveratrol induces long-lasting expression of differentiation markers in U87MG cells. U87MG cells were incubated for 96 h with 100  $\mu$ M RV (medium was changed and RV readded every 24 h), and then they were cultured in fresh RV-free medium (changed every 24 h) for the time indicated. At the time-points indicated, cells were collected and the expression of Nestin, GFAP, and  $\beta$ III tubulin mRNAs was evaluated by qRT-PCR (data of three independent experiments  $\pm$  SD;  $p < 0.05$ ). Data in this Figure have been reproduced in three independent experiments.

although a transient and limited fluctuation of GFAP mRNA was observed. In RV pretreated cells, the mRNA levels of the three

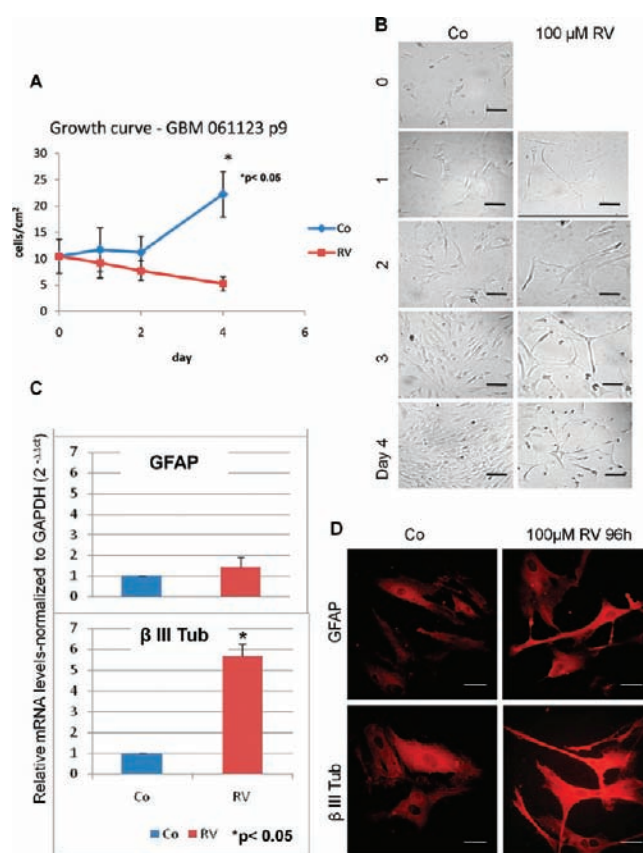


**Figure 7.** Effect of chronic exposure to resveratrol in primary human glioblastoma cells. Primary human glioblastoma cells were cultured for up to 96 h in the absence or the presence of 100  $\mu$ M RV (medium was changed and RV readded every 24 h). (A) At each time-point, the viable (trypan blue-excluding) cells were counted. (B) Representative images of cell morphology under the phase-contrast microscope (bar = 0.1 mm). (C) Quantification of the mRNA levels of GFAP and  $\beta$ III-tubulin. (D) Immunofluorescence staining of GFAP and  $\beta$  III-tubulin (bar = 0.1 mm). Data in this figure have been reproduced in three independent experiments.

markers diminished during the culture in RV-free medium. In particular, (i) nestin mRNA decreased to  $\sim$ 75% of the control value, (ii)  $\beta$ III tubulin mRNA was rapidly (in the first 24 h) down-regulated, compared to control levels. However, the GFAP mRNA level decreased only slightly, remaining about 3-fold higher than control level.

**Chronic Exposure to Resveratrol Induces Long-Lasting Expression of Differentiation Markers in Primary Human Glioblastoma Cells.** Finally, we checked whether the beneficial phenotypic changes induced by RV in U87MG cell line could be reproduced in primary cultures of human glioblastoma explants. Primary glioblastoma cells are able to reproduce in vitro and to form tumors when intracranially injected in nude mice.<sup>24,27,28</sup> We cultured human primary glioblastoma cells for up to 96 h in the absence or the presence of 100  $\mu$ M RV and looked for changes in the morphology and growth rate. RV inhibited the growth of primary glioblastoma cells and also induced cell death and acquisition of typical fusiform morphology, characterized by long cytoplasmic extensions, in the surviving cells (Figure 7A and 7B). Next, we looked at the phenotypic expression of the markers for neuronal-like and glial-like differentiation in primary glioblastoma cells exposed to RV for up to 96 h. RT-PCR analysis

of mRNA levels indicated a slight (not significant) up-regulation of GFAP expression and a consistent (~5.5 fold) up-regulation of  $\beta$ III tubulin (Figure 7C). These data were further supported by immunofluorescence staining of both markers (Figure 7D).

## DISCUSSION

RV, a natural phytoalexin, is rapidly converted into hydrophilic conjugates, which facilitates the entry in the bloodstream, can cross the blood–brain barrier, and is taken up by brain tissue,<sup>29</sup> a fact that makes this drug potentially useful in the treatment of brain tumors. Consistently, RV has been shown to suppress the angiogenesis and tumor growth of gliomas in rats.<sup>30,31</sup> These effects were observed with a daily administration of 100 mg/kg body-weight.<sup>31</sup>

In this study we demonstrate that, on chronic treatment, RV arrested cell growth, induced cell death, decreased cell migration and invasion through matrigel, and promoted long-lasting morphological changes reminiscent of a more mature phenotype. These effects were demonstrated in cultured human U87MG cells and could be reproduced in human primary glioblastoma cultures. RV induced bax-mediated apoptosis but not necrosis. This is of particular relevance for therapeutic treatments of tumors *in vivo* since it is favored for the phagocytic elimination of dead tumor cells in the absence of an inflammatory response, normally associated with necrosis, that is associated with tumor growth promotion and poor prognosis. Proliferation arrest was observed as early as after one day of treatment with RV and was enhanced with time of treatment, consistent with previous findings in rat glioma C6 cells.<sup>32</sup> We assayed the expression of Ki-67, a marker of proliferation also used as additional prognostic marker in human astrocytomas.<sup>19</sup> In cultured U87MG cells, Ki-67 was expressed in ~37% of the population, a value reported also by other authors,<sup>33</sup> and this percentage dropped to ~21% upon 48 h treatment with RV. We note that cells which survived to the chronic (96 h) treatment with RV did not rescue the ability to proliferate during 3 days of culture in RV-free medium. It is conceivable that the cells chronically treated with RV eventually underwent a process of senescence. Consistent with this hypothesis, we found that a high percentage of cells pretreated with RV and cultured for up to 3 days in RV-free medium were positive for the senescence-associated  $\beta$ -galactosidase marker.<sup>34</sup> An analogous effect was observed in RV-treated rat C6 glioma cells.<sup>35</sup> Our data demonstrate the efficacy of RV in inhibiting cell growth also in two primary cultures (only one is presented in this study) obtained from human GBM explants.

We also show that RV greatly reduces the invasive growth through Matrigel and inhibits cell migration of U87MG cells. A similar effect has been reported in hepatocarcinoma cells and has been attributed to the regulation of metalloproteases and of their inhibitors by RV.<sup>10</sup> Decreased invasion was observed within 48 h of RV treatment, at which time-point cell death was negligible, while inhibition of cell migration was evident as early as by 8 h of incubation and lasted for the subsequent 24 h. This rules out the possibility that unhealing of the wound was the consequence of the inhibition of cell proliferation (which in fact was apparent by 48 h of treatment). Consistent with this interpretation, the cyclin-dependent kinase inhibitor p21(Waf1/Cip1) started to accumulate in the cells between 24 and 36 h of incubation with RV (not shown). Given the important role of the Akt pathway in GBM cell migration and invasiveness,<sup>2,22</sup> we assayed the level of phosphorylated Akt in U87MG cells. Control cells showed basal high level of phosphorylated Akt. RV treatment elicited a prompt

and persistent down-regulation of Akt phosphorylation, which paralleled the inhibitory effect on wound-healing and matrigel invasion. A 24 h treatment with RV elicited a nearly 10-fold decrease in the amount of phosphorylated Akt in U87MG cells. Activation of the Akt pathway has been specifically implicated in the pathogenesis of glioblastomas,<sup>36</sup> as well as with chemoresistance<sup>37</sup> and increased tumorigenicity, invasiveness, and stemness.<sup>2</sup> Thus, the ability of RV to down-regulate the phosphorylation of Akt is likely to positively impact a range of phenotypic and behavioral characteristics of GBM cells.

In this study, we further show that a subpopulation of U87MG cells resisted RV toxicity and with time acquired a morphology characterized by long cytoplasmic extensions; therefore, we hypothesize that RV could also favor the differentiation of GBM cells. Reportedly, glioma stem cells characteristically express prominin 1/CD133 and nestin, along with some other markers, shared with normal neural stem cells.<sup>38</sup> Nestin is also highly expressed in U87MG-induced tumors as well as in human GBMs as compared to less malignant glioma and normal brain tissue, this protein being associated with the motility, invasive potential, and worse survival rate of patients.<sup>22,39,40</sup> The expression of GFAP, the marker of differentiated astrocytes, is very often completely lost in GBMs, similar to  $\beta$ III-tubulin, which is characteristically expressed in mature neurons. It is noticed that RV has been shown to also promote the differentiation of cultured neuroblastoma cells.<sup>41</sup> RV promoted the appearance of a more differentiated phenotype characterized by reduced expression of nestin and increased expression of GFAP and of  $\beta$ III-tubulin in cultured U87MG cells. The morphological and phenotypic changes observed under chronic administration of RV lasted for almost 4 days after removal of the drug. The efficacy of RV in inhibiting cell growth and inducing neuronal- and glial-like differentiation was further confirmed in primary cultures from human glioblastomas explants. It should be stressed that this is the first study showing such effect of RV in glioblastoma cells. These findings support the introduction of pulsed administration of this food-derived molecule in the chemotherapy regimen of astrocytomas. In this respect, it should be noted that after a dose of 30 mg/kg body-weight, the concentration of RV in the brain tissue of gerbils was found in the nanomolar range,<sup>29</sup> whereas the antitumor effects in cultured GBM cells described in the literature and in this work were seen for concentrations of RV in the micromolar range. Yet the intraperitoneal injection of 30 mg/kg RV elicited hippocampal neuron protection from ischemia toxicity in gerbils,<sup>29</sup> and a daily administration of 100 mg/kg RV reduced the growth of intracerebral implanted gliomas and prolonged the survival in rats after a 4-week treatment.<sup>31</sup> These data suggest that *in vivo* the antitumor effects of RV can be obtained at concentrations lower than those used *in vitro*. At any rate, the introduction in therapy of specific drug carriers, e.g., nanoparticles,<sup>42</sup> could facilitate the accumulation of sufficient bioactive RV in the affected brain.

## AUTHOR INFORMATION

### Corresponding Author

\*Fax: ++39-0321-620421; e-mail: isidoro@med.unipmn.it.

### Author Contributions

<sup>5</sup>These authors equally contributed to the work.

### Funding Sources

This work was supported by grants from Fondazione Cassa di Risparmio di Torino, Compagnia San Paolo di Torino (progetto

Neuroscienze 2008.2395), and Regione Piemonte (Ricerca Sanitaria Finalizzata) (to C.I.), and by grants from Slovenian Research Agency (P1-0245 to T.L.). R. Veneroni is recipient of a Ph.D. fellowship sponsored by Comoli-Ferrari & C. SpA (Novara, Italy).

## ACKNOWLEDGMENTS

The authors are grateful to Prof. D. Schiffer (Centro di Neuro-Bio-Oncologia, Vercelli, Italy) for advices and helpful discussion.

## ABBREVIATIONS USED

GBM, glioblastoma; GFAP, glial fibrillary acidic protein; RV, resveratrol; WHO, World Health Organization

## REFERENCES

- Ohgaki, H.; Kleihues, P. Genetic alterations and signaling pathways in the evolution of gliomas. *Cancer Sci.* **2009**, *100*, 2235–41.
- Molina, J. R.; Hayashi, Y.; Stephens, C.; Georgescu, M. M. Invasive glioblastoma cells acquire stemness and increased Akt activation. *Neoplasia* **2010**, *12*, 453–63.
- Suzuki, Y.; Shirai, K.; Oka, K.; Mobaraki, A.; Yoshida, Y.; Noda, S. E.; Okamoto, M.; Suzuki, Y.; Itoh, J.; Itoh, H.; Ishiuchi, S.; Nakano, T. Higher pAkt expression predicts a significant worse prognosis in glioblastomas. *J. Radiat. Res. (Tokyo)* **2010**, *51*, 343–8.
- Johannessen, T. C.; Bjerkvig, R.; Tysnes, B. B. DNA repair and cancer stem-like cells—potential partners in glioma drug resistance? *Cancer Treat. Rev.* **2008**, *34*, 558–67.
- Signorelli, P.; Ghidoni, R. Resveratrol as an anticancer nutrient: molecular basis, open questions and promises. *J. Nutr. Biochem.* **2005**, *16*, 449–66.
- Aggarwal, B. B.; Bhardwaj, A.; Aggarwal, R. S.; Seeram, N. P.; Shishodia, S.; Takada, Y. Role of resveratrol in prevention and therapy of cancer: preclinical and clinical studies. *Anticancer Res.* **2004**, *24*, 2783–840.
- Jang, M.; Cai, L.; Udeani, G. O.; Slowing, K. V.; Thomas, C. F.; Beecher, C. W.; Fong, H. H.; Farnsworth, N. R.; Kinghorn, A. D.; Mehta, R. G.; Moon, R. C.; Pezzuto, J. M. Cancer chemopreventive activity of resveratrol, a natural product derived from grapes. *Science* **1997**, *275*, 218–20.
- Banerjee, S.; Bueso-Ramos, C.; Aggarwal, B. B. Suppression of 7,12 dimethylbenz(a)anthracene-induced mammary carcinogenesis in rats by resveratrol: role of nuclear factor-kappaB, cyclooxygenase 2, and matrix metalloproteinase 9. *Cancer Res.* **2002**, *62*, 4945–54.
- Ahmad, N.; Adhami, V. M.; Afaq, F.; Feyes, D. K.; Mukhtar, H. Resveratrol causes WAF-1/p21 mediated G(1)-phase arrest of cell cycle and induction of apoptosis in human epidermoid carcinoma A431 cells. *Clin. Cancer Res.* **2001**, *7*, 1466–73.
- Weng, C. J.; Wu, C. F.; Huang, H. W.; Wu, C. H.; Ho, C. T.; Yen, G. C. Evaluation of anti-invasion effect of resveratrol and related methoxy analogues on human hepatocarcinoma cells. *J. Agric. Food Chem.* **2010**, *58* (5), 2886–94.
- Tinhofer, I.; Bernhard, D.; Senfter, M.; Anether, G.; Loeffler, M.; Kroemer, G.; Kofler, R.; Csordas, A.; Greil, R. Resveratrol, a tumor-suppressive compound from grapes, induces apoptosis via a novel mitochondrial pathway controlled by Bcl-2. *FASEB J.* **2001**, *15*, 1613–5.
- Trincheri, N. F.; Nicotra, G.; Follo, C.; Castino, R.; Isidoro, C. Resveratrol induces cell death in colorectal cancer cells by a novel pathway involving lysosomal cathepsin D. *Carcinogenesis* **2007**, *28*, 922–31.
- Scarlatti, F.; Maffei, R.; Beau, I.; Codogno, P.; Ghidoni, R. Role of non-canonical Beclin 1-independent autophagy in cell death induced by resveratrol in human breast cancer cells. *Cell Death Differ.* **2008**, *15*, 1318–29.
- Trincheri, N. F.; Follo, C.; Nicotra, G.; Peracchio, C.; Castino, R.; Isidoro, C. Resveratrol-induced apoptosis depends on the lipid kinase activity of Vps34 and on the formation of autophagolysosomes. *Carcinogenesis* **2008**, *29*, 381–9.
- Boocock, D. J.; Faust, G. E.; Patel, K. R.; Schinas, A. M.; Brown, V. A.; Ducharme, M. P.; Booth, T. D.; Crowell, J. A.; Perloff, M.; Gescher, A. J.; Steward, W. P.; Brenner, D. E. Phase I dose escalation pharmacokinetic study in healthy volunteers of resveratrol, a potential cancer chemopreventive agent. *Cancer Epidemiol. Biomarkers Prev.* **2007**, *16*, 1246–52.
- Cottart, C. H.; Nivet-Antoine, V.; Laguillier-Morizot, C.; Beaudeau, J. L. Resveratrol bioavailability and toxicity in humans. *Mol. Nutr. Food Res.* **2010**, *54*, 7–16.
- Pucer, A.; Castino, R.; Mirković, B.; Falnoga, I.; Slejkovec, Z.; Isidoro, C.; Lah, T. T. Differential role of cathepsins B and L in autophagy-associated cell death induced by arsenic trioxide in U87 human glioblastoma cells. *Biol. Chem.* **2010**, *391*, 519–31.
- Gole, B.; Durán Alonso, M. B.; Dolenc, V.; Lah, T. Post-translational regulation of cathepsin B, but not of other cysteine cathepsins, contributes to increased glioblastoma cell invasiveness in vitro. *Pathol. Oncol. Res.* **2009**, *15*, 711–23.
- Johannessen, A. L.; Torp, S. H. The clinical value of Ki-67/MIB-1 labeling index in human astrocytomas. *Pathol. Oncol. Res.* **2006**, *12*, 143–7.
- Chin, Y. R.; Toker, A. Function of Akt/PKB signaling to cell motility, invasion and the tumor stroma in cancer. *Cell Signal* **2009**, *21*, 470–6.
- Joy, A. M.; Beaudry, C. E.; Tran, N. L.; Ponce, F. A.; Holz, D. R.; Demuth, T.; Berens, M. E. Migrating glioma cells activate the PI3-K pathway and display decreased susceptibility to apoptosis. *J. Cell Sci.* **2003**, *116*, 4409–17.
- Ma, Y. H.; Mentlein, R.; Knerlich, F.; Kruse, M. L.; Mehdorn, H. M.; Held-Feindt, J. Expression of stem cell markers in human astrocytomas of different WHO grades. *J. Neurooncol.* **2008**, *86*, 31–45.
- Singh, S. K.; Clarke, I. D.; Hide, T.; Dirks, P. B. Cancer stem cells in nervous system tumors. *Oncogene* **2004**, *23*, 7267–73.
- Wang, J.; Sakariassen, P. Ø.; Tsinkalovsky, O.; Immervoll, H.; Bøe, S. O.; Svendsen, A.; Prestegarden, L.; Røslund, G.; Thorsen, F.; Stuhr, L.; Molven, A.; Bjerkvig, R.; Enger, P. Ø. CD133 negative glioma cells form tumors in nude rats and give rise to CD133 positive cells. *Int. J. Cancer* **2008**, *122*, 761–8.
- Lendahl, U.; Zimmerman, L. B.; McKay, R. D. CNS stem cells express a new class of intermediate filament protein. *Cell* **1990**, *60*, 585–95.
- Jiang, Y. Q.; Oblinger, M. M. Differential regulation of beta III and other tubulin genes during peripheral and central neuron development. *J. Cell Sci.* **1992**, *103*, 643–51.
- Beier, D.; Hau, P.; Proescholdt, M.; Lohmeier, A.; Wischhusen, J.; Oefner, P. J.; Aigner, L.; Brawanski, A.; Bogdahn, U.; Beier, C. P. CD133(+) and CD133(-) glioblastoma-derived cancer stem cells show differential growth characteristics and molecular profiles. *Cancer Res.* **2007**, *67*, 4010–5.
- Joo, K. M.; Kim, S. Y.; Jin, X.; Song, S. Y.; Kong, D. S.; Lee, J. I.; Jeon, J. W.; Kim, M. H.; Kang, B. G.; Jung, Y.; Jin, J.; Hong, S. C.; Park, W. Y.; Lee, D. S.; Kim, H.; Nam, D. H. Clinical and biological implications of CD133-positive and CD133-negative cells in glioblastomas. *Lab Invest.* **2008**, *88*, 808–15.
- Wang, Q.; Xu, J.; Rottinghaus, G. E.; Simonyi, A.; Lubahn, D.; Sun, G. Y.; Sun, A. Y. Resveratrol protects against global cerebral ischemic injury in gerbils. *Brain Res.* **2002**, *958*, 439–47.
- Kimura, Y.; Sumiyoshi, M.; Baba, K. Antitumor activities of synthetic and natural stilbenes through antiangiogenic action. *Cancer Sci.* **2008**, *99*, 2083–96.
- Tseng, S. H.; Lin, S. M.; Chen, J. C.; Su, Y. H.; Huang, H. Y.; Chen, C. K.; Lin, P. Y.; Chen, Y. Resveratrol suppresses the angiogenesis and tumor growth of gliomas in rats. *Clin. Cancer Res.* **2004**, *10*, 2190–202.
- Zhang, W.; Fei, Z.; Zhen, H. N.; Zhang, J. N.; Zhang, X. Resveratrol inhibits cell growth and induces apoptosis of rat C6 glioma cells. *J. Neurooncol.* **2007**, *81*, 231–40.



(33) Annabi, B.; Lachambre, M. P.; Plouffe, K.; Sartelet, H.; Béliveau, R. Modulation of invasive properties of CD133+ glioblastoma stem cells: a role for MT1-MMP in bioactive lysophospholipid signaling. *Mol. Carcinog.* **2009**, *48*, 910–9.

(34) Dimri, G. P.; Lee, X.; Basile, G.; Acosta, M.; Scott, G.; Roskelley, C.; Medrano, E. E.; Linskens, M.; Rubelj, I.; Pereira-Smith, O.; Peacocket, M.; Campisi, J. A biomarker that identifies senescent human cells in culture and in aging skin in vivo. *Proc. Natl. Acad. Sci. U.S.A.* **1995**, *92*, 9363–7.

(35) Zamin, L. L.; Filippi-Chiela, E. C.; Dillenburger-Pilla, P.; Horn, F.; Salbego, C.; Lenz, G. Resveratrol and quercetin cooperate to induce senescence-like growth arrest in C6 rat glioma cells. *Cancer Sci.* **2009**, *100*, 1655–62.

(36) Sonoda, Y.; Ozawa, T.; Aldape, K. D.; Deen, D. F.; Berger, M. S.; Pieper, R. O. Akt pathway activation converts anaplastic astrocytoma to glioblastoma multiforme in a human astrocyte model of glioma. *Cancer Res.* **2001**, *61*, 6674–8.

(37) Li, B.; Chang, C. M.; Yuan, M.; McKenna, W. G.; Shu, H. K. Resistance to small molecule inhibitors of epidermal growth factor receptor in malignant gliomas. *Cancer Res.* **2003**, *63*, 7443–50.

(38) Singh, S. K.; Clarke, I. D.; Terasaki, M.; Bonn, V. E.; Hawkins, C.; Squire, J.; Dirks, P. B. Identification of a cancer stem cell in human brain tumors. *Cancer Res.* **2003**, *63*, 5821–8.

(39) Rutka, J. T.; Ivanchuk, S.; Mondal, S.; Taylor, M.; Sakai, K.; Dirks, P.; Jun, P.; Jung, S.; Becker, L. E.; Ackerley, C. Co-expression of nestin and vimentin intermediate filaments in invasive human astrocytoma cells. *Int. J. Dev. Neurosci.* **1999**, *17*, 503–15.

(40) Strojnik, T.; Røsland, G. V.; Sakariassen, P. O.; Kavalari, R.; Lah, T. Neural stem cell markers, nestin and musashi proteins, in the progression of human glioma: correlation of nestin with prognosis of patient survival. *Surg. Neurol.* **2007**, *68*, 133–43.

(41) Melzig, M. F.; Escher, F. Induction of neutral endopeptidase and angiotensin-converting enzyme activity of SK-N-SH cells in vitro by quercetin and resveratrol. *Pharmazie* **2002**, *57*, 556–8.

(42) Shao, J.; Li, X.; Lu, X.; Jiang, C.; Hu, Y.; Li, Q.; You, Y.; Fu, Z. Enhanced growth inhibition effect of resveratrol incorporated into biodegradable nanoparticles against glioma cells is mediated by the induction of intracellular reactive oxygen species levels. *Colloids Surf., B* **2009**, *71*, 40–7.